A New Approach to Estimating Rainwater Content by Radar Using Propagation Differential Phase Shift

A. R. JAMESON

Applied Research Corporation, Landover, Maryland

I. J. CAYLOR*

Department of Electrical Engineering, Colorado State University, Fort Collins, Colorado

(Manuscript received 14 December 1992, in final form 16 June 1993)

ABSTRACT

As microwaves propagate through rain, the rate of phase change with increasing distance is different depending upon whether the transmissions are polarized horizontally or vertically. This rate of change is the so-called specific propagation differential phase shift Φ_{DP}. This paper demonstrates that at several frequencies and over a wide domain the ratio of Φ_{DP} to the rainwater content W is nearly linearly related to D_m, the mass-weighted mean drop size. An investigation of errors indicates that this new approach is likely to yield more accurate estimates of W than the other classical reflectivity factor Z, attenuation, or polarization techniques. The most accurate estimates of W are most likely at the highest frequency considered, 13.80 GHz.

In lieu of such high-frequency measurements, these somewhat esoteric results are made more concrete through an analysis of 3-GHz radar measurements collected during the Convection and Precipitation Experiment in a tropical rainstorm in Florida. Among the principle advantages of using Φ_{DP} to measure rain are that an absolute calibration of the radar is no longer required and the estimates are decoupled from measurements of the radar reflectivity factor. Consequently, temporal and spatial structures of rain estimates do not simply mimic those of the reflectivity factor, as happens for classical estimation techniques using Z.

1. Introduction

As quiescent raindrops fall, they assume the ubiquitous and well-known "equilibrium" shape originally described from wind tunnel observations of Pruppacher and Beard (1970) in which the drops are nearly oblate spheroids with the major axis in the horizontal and the minor axis, as well as the axis of symmetry, in the vertical. The raindrops, therefore, affect microwave transmissions differently depending upon whether the polarization is vertical or horizontal. This asymmetry in the medium, in turn, produces different backscattered powers, specific attenuations, and specific phases between transmissions at these two polarizations. While a source of consternation to the communications industry, these differences provide potentially valuable information for improving quantitative radar rain measurements.

A particularly interesting parameter is the rate of change of the difference in phase between vertically and horizontally polarized waves as they propagate through rain. This specific propagation differential phase shift Φ_{DP} is closely related to the rainfall rate in still air R (Sachidananda and Zrnić 1986a; Chandrasekar et al. 1990; Jameson 1991; Jameson 1994b). It is also a strong function of the rainwater content W (Jameson 1985) through relations such as

$$W = \left[\frac{\Phi_{DP}}{(1 - Я)}\right]^q, \tag{1}$$

where $Я$ is the mass-weighted mean axis ratio (r—minor axis/major axis) and q ranges from approximately 0.9 to 0.96 (Jameson 1994a).

Examples of these latter expressions for 3 and 13 GHz are shown in Fig. 1 for an ensemble of gamma drop size distributions (Ulbrich 1983) of the form

$$N(D) = N_0 D^{\mu} e^{-\Lambda D}, \tag{2}$$

where $N(D)dD$ is the concentration of drops of size D to $D + dD$, and Λ is the slope of the distribution. In these examples, $-1 \leq \mu \leq 2$, $16 \leq \Lambda \leq 45$ cm^{-1}, and N_0 is chosen to be consistent with a rainfall rate specified by Λ for the Sekhon and Srivastava (1971) family of thunderstorm drop size distributions. Obviously, in Fig. 1 the quantities are highly correlated and yield least-squares-error fits having small average standard errors of ±10% at 13 GHz and ±14% at 3 GHz. In practice, however, these errors will not be random in

* Current affiliation: Science Systems and Applications, Inc., Lanham, Maryland.

Corresponding author address: Dr. A. R. Jameson, Applied Research Corporation, 8201 Corporate Drive, Landover, MD 20785.

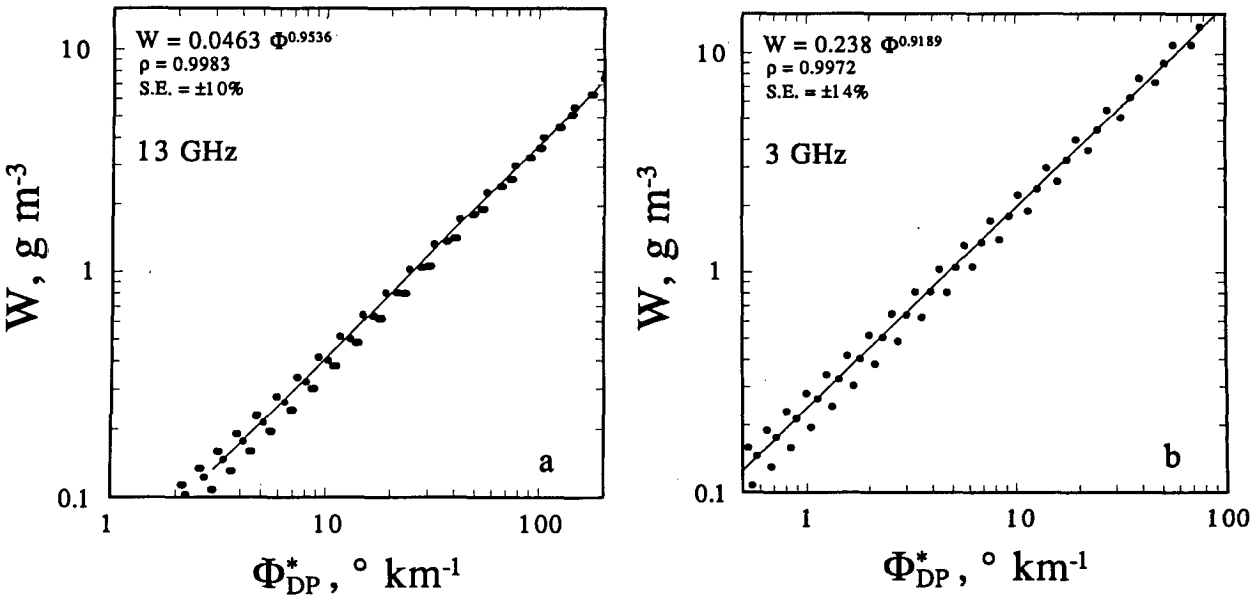

FIG. 1. Correlation coefficient ρ, standard error SE, and least-squares-error fit between the rainwater content W and the modified rate of polarization differential phase shift Φ^*_{DP} at (a) 13.80 GHz and (b) 2.80 GHz for an ensemble of gamma drop size distributions and temperatures of 0°, 10°, 20°, and 30°C. Here, $\Phi^*_{DP} = \Phi_{DP}/(1 - Я)$, where Φ_{DP} is the specific polarization differential phase shift and $Я$ is the mass-weighted mean axis ratio of the equilibrium shaped drops.

time or space so that they represent average potential bias errors. In an attempt to reduce such errors even further, an alternative approach is explored in this paper.

2. Theory

Since the state of polarization of plane waves is two-dimensional, the waves scattered by precipitation, for example, are related to the transmitted waves through a two-dimensional scattering matrix **S**. Since scattering depends on direction, one **S**, for example, corresponds to backscatter ($\mathbf{S}_b$), while another corresponds to forward scatter ($\mathbf{S}_f$). Van de Hulst (1957) shows that with increasing distance the rate of (or "specific") attenuation is then related to the ensemble of scatterers by [expressed here using the convention of Oguchi (1973)]

$$A_{H,V} = 0.4343\lambda \int \mathrm{Im}[S_f(D)_{H,V}]N(D)dD, \quad (3)$$

where $A_{H,V}$ is the specific attenuation at horizontal or vertical polarization, λ is the wavelength, and Im is the imaginary component of $\mathbf{S}_f$. Similarly, the specific phase change is given by

$$\Phi_{H,V} = \frac{180 \times 10^{-1}}{\pi} \int \mathrm{Re}[S_f(D)_{H,V}]N(D)dD, \quad (4)$$

where the integral is over all of the drops in the distribution and Re is the real component of $\mathbf{S}_f$.

The real and imaginary components of $\mathbf{S}_f$ are functions of both the drop size and drop shape as well as the frequency and the temperature. At frequencies below around 20 GHz, Atlas and Ulbrich (1974) show that for spherical drops $\mathrm{Im}(\mathbf{S}_f) \approx C_A D^4$. Similarly, Jameson (1989) shows that for frequencies less than about 15 GHz, $\mathrm{Re}(\mathbf{S}_f) \approx C_\Phi D^3$ for water spheres. In addition, for frequencies from 3 to 15 GHz, Jameson (1989) shows that the effects of raindrop size and shapes can be separated so that for each drop

$$\mathrm{Im}(S_f)_H \approx C_A[1 + (1 - r)]D^4,$$
$$\mathrm{Im}(S_f)_V \approx C_A[1 - (1 - r)]D^4, \quad (5)$$

where r is the drop axis ratio. Similarly,

$$\mathrm{Re}(S_f)_H \approx C_\Phi[1 + (1 - r)]D^3,$$
$$\mathrm{Re}(S_f)_V \approx C_\Phi[1 - (1 - r)]D^3. \quad (6)$$

Substituting (5) and (6) into (3) and (4) yields

$$A_{H-V} \approx 2C_A W D_m(1 - \mathcal{R}) \quad (7)$$

and

$$\Phi_{DP} \approx 2C_\Phi W(1 - Я), \quad (8)$$

where

$$D_m = \frac{\int D^4 N(D)dD}{\int D^3 N(D)dD} \quad (9a)$$

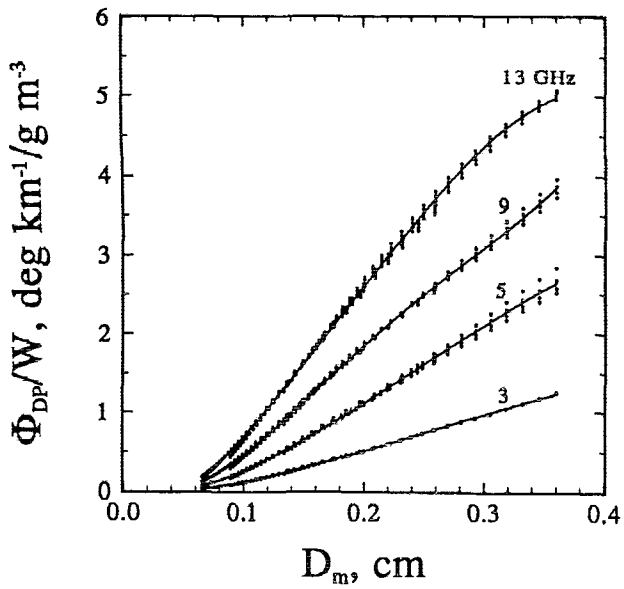

FIG. 2. The ratio of the specific polarization differential phase shift to rainwater content W as a function of the mass-weighted mean drop diameter and for frequencies of 13.80 (13), 9.34 (9), 5.48 (5), and 2.80 (3) GHz. The fitted curves are in Table 1.

and

$$\mathcal{R} = \frac{\int rD^4N(D)dD}{\int D^4N(D)dD}, \tag{9b}$$

$$\mathcal{Z} = \frac{\int rD^3N(D)dD}{\int D^3N(D)dD}. \tag{9c}$$

For equilibrium shaped drops, Pruppacher and Beard (1970) show, to a good approximation, that

$$r = 1.03 - 0.62D, \tag{10}$$

where D is in centimeters. From (9a) and (9c) it is easy then to show from (8) that

$$\frac{\Phi_{DP}}{W} \approx C_\Phi(0.62D_m - 0.03); \tag{11}$$

that is, Φ_{DP}/W is a linear function of D_m regardless of the form of the drop size distribution. Except for different coefficients, the same is also true for any other nonequilibrium but linear drop size–shape relation as well.

Figure 2 illustrates that the linearity implied by (11) is maintained at several frequencies over a wide domain of D_m. The quantities in Fig. 2 are calculated for the ensemble of drop size distributions mentioned previously and for $\mathbf{S}_f$ computed for temperatures of 0°, 10°, . . . , 30°C using the program of Warner and Hizal (1976) based on the matrix technique of Waterman (1965). Ironically, although the temperature has only a minor effect on Re($\mathbf{S}_f$) (Jameson 1992), most of the scatter in Fig. 2 arises from temperature differences. Very little scatter is produced by the different forms of the gamma drop size distributions. However, because (5)–(6) are only approximations to the more detailed expressions in Jameson (1989), nonlinearities do appear particularly at large D_m. To include these slight deviations, highly correlated least-squares-error polynomial fits corresponding to the curves in Fig. 2 are computed and listed in Table 1.

To use these relations to compute W from Φ_{DP}, it is necessary to estimate D_m first. At frequencies that attenuate significantly in rain (e.g., 9 and 13 GHz), one approach (Jameson 1994a) is to combine (7) and (8) so that

$$\frac{A_{H-V}}{\Phi_{DP}} \approx CD_m\mathfrak{R}, \tag{12}$$

where C is a constant and $\mathfrak{R} = (1 - \mathcal{R})/(1 - \mathcal{Z})$. It is easy to show for linear size–shape relations that $\mathcal{R} = 1.03 - 0.62(5 + \mu)/\Lambda$, while $\mathcal{Z} = 1.03 - 0.62(4 + \mu)/\Lambda$ for gamma drop size distributions integrated over $0 \leq D \leq \infty$, for example. Thus, the ratio $\mathfrak{R}$ is a well-behaved, slowly varying function of both Λ and μ, and it should be possible to estimate D_m using A_{H-V}/Φ_{DP}. This is illustrated in Fig. 3 for frequencies of 9.34 and 13.80 GHz.

For transmissions at lower frequencies (e.g., 5 and 3 GHz), attenuation is too weak to estimate A_{H-V} and, hence, D_m using (12). At 3 GHz one option is to use the differential reflectivity Z_{DR} to estimate D_m. Seliga and Bringi (1976) define the differential reflectivity (in its antilog form) as the ratio of the radar reflectivity factor at horizontal polarization (Z_H) to that at vertical

TABLE 1. The coefficients of polynomial fits between the ratio Φ_{DP}/W and the mass-weighted mean diameter D_m of the form $\Phi_{DP}/W = C_4D_m^4 + C_3D_m^3 + C_2D_m^2 + C_1D_m + C_0$ over the ensemble of drop size distributions and temperatures given in the text. Here, r is the correlation coefficient.

Frequency (GHz)	C_4	C_3	C_2	C_1	C_0	r
13.80	0.0	−133.9015	71.17706	7.25874	−0.6096467	0.9994
9.34	668.3916	−606.8504	189.3342	−10.37487	0.1429265	0.9995
5.48	0.0	−53.16749	38.93155	0.621036	−0.1370949	0.9987
2.80	0.0	−19.69431	15.41786	0.6820518	−0.08446753	0.9996

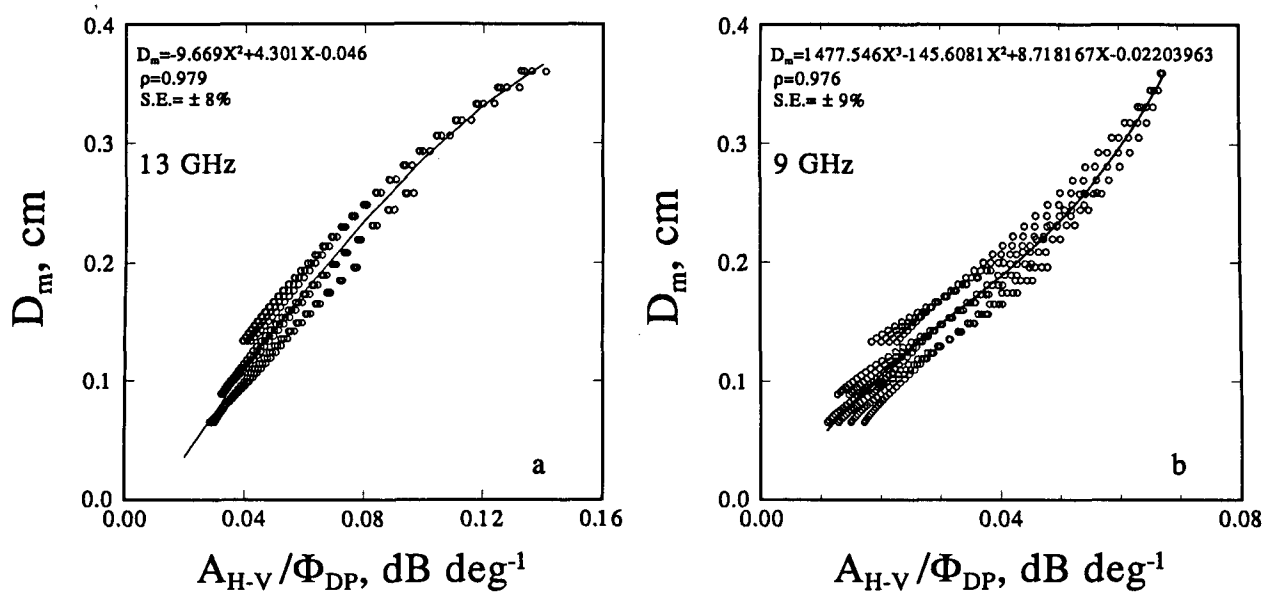

FIG. 3. The correlation coefficient ρ, standard error, and least-squares-error polynomial fit between the mass-weighted mean drop diameter D_m and the ratio of the specific polarization differential attenuation to the specific polarization propagation differential phase shift at (a) 13.80 GHz and (b) 9.34 GHz for the ensemble of gamma drop size distributions and temperatures discussed in the text.

polarization (Z_V); that is, $\zeta = Z_H/Z_V$. Because the differential reflectivity is a measure of the *reflectivity*-weighted mean axis ratio of the raindrops (Jameson 1983), ζ is most strongly influenced by the large raindrops whereas D_m is less so. Nevertheless, at least within the confines of the forms of the drop size distribution selected for this study, Fig. 4 illustrates that ζ can be used to estimate D_m reasonably well. However, it is worth noting that an addition of spherical drops affects ζ but not the ratio A_{H-V}/Φ_{DP}.

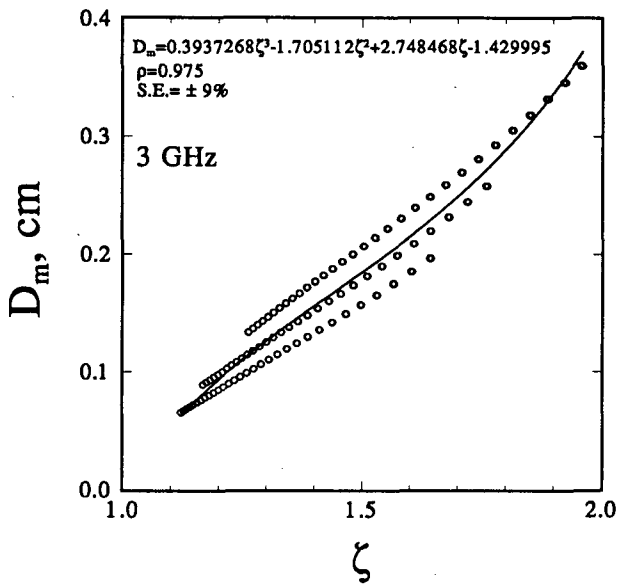

FIG. 4. The correlation coefficient ρ, standard error, and least-squares-error polynomial fit between the mass-weighted mean drop diameter, and the antilog ζ of the differential reflectivity Z_{DR} at 2.80 GHz for the ensemble of gamma drop size distributions and temperatures discussed in the text.

For an historical perspective, it is worth noting that Seliga and Bringi (1978) suggest a method for computing (not measuring) any integral parameter of an assumed size distribution. By using Z_{DR} and Φ_{DP} to estimate the median volume diameter D_0 (which divides the water content equally between drops greater than D_0 and those smaller than D_0) as well as the constant N_0 for an assumed exponential form [$\mu = 0$ in (2)] of the drop size distribution having $0 \leq D \leq \infty$ (so-called infinite distributions), it is then possible to specify (2) explicitly so that any integral parameter can be calculated.

It is important to point out that the method described in this paper goes well beyond such an expedient but unilluminating approach. First, the expressions in Table 1 and Fig. 3 can be used *directly* to estimate W and D_m without requiring the data to fit an assumed "infinite" exponential drop size distribution. The results here apply to a wide variety of frequencies and drop size distributions. Second, this study uses D_m rather than D_0. Except for the trivial case of monodisperse drop size distributions, it is easy to demonstrate and important to note that D_0 does *not* equal D_m, which arises naturally from scattering theory. The selection of D_0 by Seliga and Bringi (1978), although stemming from historical precedence, is an arbitrary choice with regard to scattering. Consequently, D_m is not only preferable for a consistent theoretical treatment, it is also

likely to yield better results than any other arbitrary diameter such as D_0.

It appears theoretically possible, therefore, potentially to improve the estimates of the rainwater content at several frequencies using the expressions in Table 1. In the next section this qualitative assertion is investigated more quantitatively, and the results using this method are compared to those from other radar water content estimation techniques.

3. Error discussion and comparisons

The accuracy of the water content estimators depends upon their mathematical expressions, their sensitivity to the form of the drop size distribution, and measurement errors. While many factors influence real radar measurements, a complete treatment of such effects is well beyond the scope of this work. Rather the focus in this section is largely on the errors generated by theoretical differences such as the slopes of the least-squares-error fits and the average scatter about these fits deduced using the selected ensemble of drop size distributions and temperatures. Standard measurement errors, however, are included as well. Consequently, it is necessary to specify these latter errors for Z_{DR}, Z_H, A_H, Φ_{DP}, and $X = A_{H-V}/\Phi_{DP}$.

In particular, the statistics of Z_{DR} are now well known (Sachidananda and Zrnić 1986a). As the number of independent samples increases, the measurement uncertainty ΔZ_{DR} approaches ±0.1 dB (i.e., $|\Delta\zeta/\zeta| \rightarrow 0.023$). Similarly, the statistical uncertainty $\Delta Z_H \rightarrow 0.5$ dBZ. However, because it is very difficult to determine the absolute radar calibration to within ±0.5 dB as well; ΔZ_H is taken here to be ±1.0 dB.

The specific propagation differential phase shift is estimated as one-half the difference in the total integrated differential phase φ_{DP} at two locations separated by distance δr (Jameson 1985; Bringi et al. 1990) as described in the Appendix. Consequently, it is easy to show that $\Delta\varphi_{DP}/\varphi_{DP} = \Delta\Phi_{DP}/\Phi_{DP}$; that is, the fractional errors of the integrated and specific differential phase are equivalent. Since $\Delta\varphi_{DP}$ is proportional to $N^{-1/2}$ where N is the number of independent samples (e.g., Sachidananda and Zrnić 1986a) and since N is proportional to frequency υ (e.g., Atlas 1964), $\Delta\varphi_{DP} \propto \upsilon^{1/2}$. On the other hand, Φ_{DP} and, consequently, $\varphi_{DP} \propto \upsilon$, so that

$$\left(\frac{\Delta\Phi_{DP}}{\Phi_{DP}}\right)_2 = \left(\frac{\upsilon_1}{\upsilon_2}\right)^{3/2}\left(\frac{\Delta\Phi_{DP}}{\Phi_{DP}}\right)_1, \qquad (13a)$$

where the subscripts refer to two different frequencies, υ_1 and υ_2. A similar argument can be made for the integrated differential attenuation as well except that calculations show that $A_{H-V} \propto \upsilon^2$ approximately. Consequently,

$$\left(\frac{\Delta A_{H-V}}{A_{H-V}}\right)_2 = \left(\frac{\upsilon_1}{\upsilon_2}\right)^{5/2}\left(\frac{\Delta A_{H-V}}{A_{H-V}}\right)_1. \qquad (13b)$$

Furthermore, since $X = A_{H-V}/\Phi_{DP}$, it is obvious that $\Delta X/X = \Delta\Phi_{DP}/\Phi_{DP} + \Delta A_{H-V}/A_{H-V}$. Thus, when $\Delta\Phi_{DP}/\Phi_{DP} = \pm 0.1$ at 2.8 GHz, the corresponding fractional errors at 9.34 and 13.80 GHz are about ±0.02 and ±0.01, respectively. If it is also assumed that $\Delta A_{H-V}/A_{H-V} = \pm 0.08$ (about four times larger than $\Delta\zeta/\zeta$) at 9 GHz, then it follows that $\Delta X/X$ is ±0.10 and ±0.04 at 9.34 and 13.80 GHz, respectively. Under these assumptions it is now reasonable to compare this approach at several different frequencies as well as to compare it to several other different estimators both including and excluding measurement errors.

Letting $D_m = G(X)$ where $X = \Delta A_{H-V}/\Phi_{DP}$ at 9 and 13 GHz ($X = \zeta$ at 3 GHz) and $\Phi_{DP}/W = F(D_m)$, then the errors associated with the estimate of W from the expressions in Table 1 are given by

$$\frac{\Delta D_m}{D_m} = \frac{X(dG/dX)}{G}\frac{dX}{X} + \epsilon_G, \qquad (14a)$$

while

$$\frac{\Delta W}{W} = \frac{\Delta\Phi_{DP}}{\Phi_{DP}} + \frac{D_m(dF/dD_m)}{F}\frac{\Delta D_m}{D_m} + \epsilon_F, \qquad (14b)$$

where ϵ_F and ϵ_G are average scatter plus bias errors associated with F and G, respectively, over the ensemble of drop size distributions and temperatures described earlier. Measurement errors enter through $\Delta X/X$ and $\Delta\Phi_{DP}/\Phi_{DP}$.

In the absence of measurement errors ($\Delta X/X = 0$), $\Delta D_m/D_m = \epsilon_G$ as shown in Fig. 5a. Obviously $\Delta D_m/D_m$ are about the same for 3, 9, and 13 GHz with progressively improving estimates as D_m increases. When measurement errors are included (Fig. 5b), the results at 13 and 3 GHz are still quite comparable provided ΔZ_{DR} is on the order of ±0.1 dB. Results at 13 GHz, however, are noticeably better than those at 9 GHz for $D_m \geq 0.2$ cm.

Similarly, in the absence of measurement errors ($\Delta X = 0$, $\Delta\Phi_{DP} = 0$), $\Delta W/W = \epsilon_G + \epsilon_F$ as illustrated in Fig. 6a. Once again, the errors at all frequencies appear comparable and exhibit a sharp increase for $D_m \leq 0.1$ cm when the polarization signals become weak. Figure 6b shows that when measurement errors are included, the dispersion of the curves increases significantly so that the best results occur at 13 GHz followed by 9 and finally 3 GHz.

While the precise magnitude of the errors in Fig. 6 should not be used dogmatically, the curves probably reflect a reasonable stratification of results according to frequency. Just as important, however, is the question of how well this approach compares to alternative radar rainfall estimation techniques. To address this, four other approaches are included. The first is a classical Z–W technique using the relations of Sekhon and Srivastava (1971) such that $W = 9.80 \times 10^{-4} Z^{0.696}$, where W is in grams per cubic meter and Z has its

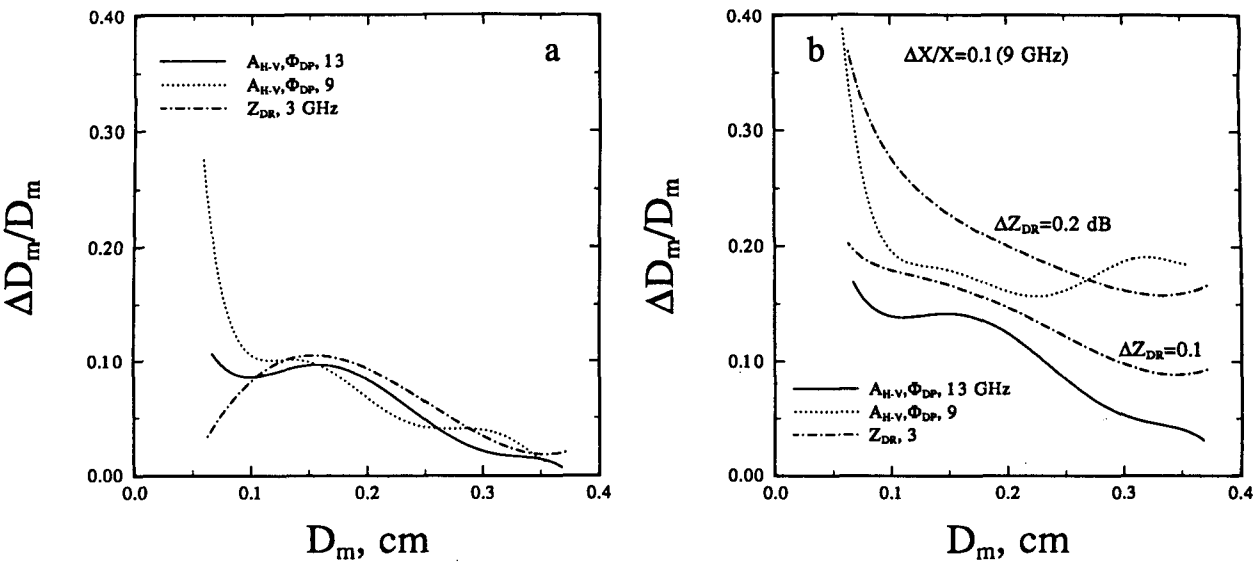

FIG. 5. The average fractional error of the estimate of D_m for the indicated algorithms (a) excluding measurement errors and (b) with measurement errors as indicated and discussed further in the text where $X = A_{H-V}/\Phi_{DP}$.

standard units ($mm^6\ m^{-3}$), respectively. Next, the two power laws in Fig. 1 having the form $W = C\Phi_{DP}^{*p}$, where $\Phi_{DP}^* = \Phi_{DP}/(1 - Я)$ are included for frequencies of 13 and 3 GHz. The approach using Z_{DR} and Z_{3H} as described in Seliga et al. (1986) is also included. However, the relations given by Seliga et al. are based upon disdrometer measurements. Calculations reveal significant bias errors when the formulas are applied directly to the ensemble of drop size distributions used in this study. To minimize such bias errors for a more objective comparison, the approach of Seliga et al. (1986) is reformulated as shown in Fig. 7. Finally, W is estimated using the W–A_H relation at 9.34 GHz as proposed by Eccles and Mueller (1971). Here, $\Delta A_H/A_H$ is taken to be ±0.08.

Regardless of approach, however, estimates corresponding to the ensemble of drop size distributions are scattered about each expression even in the absence of measurement error. In general this scatter consists of biased (ϵ_B) and unbiased (ϵ_S) components. The $\Delta W/W$ over the ensemble of distributions are scattered. Here, ϵ_B is parameterized as the least-squares-error fit to $\Delta W/W$ as a function of D_m, while ϵ_S is parameterized as the least-squares-error fit to the residual difference between the scattered $\Delta W/W$ and ϵ_B. In Fig. 8a, even without measurement error (but including biases in estimating D_m when relevant), the most biased estimators of W are the Z–W and W–A_H relations. The W–Φ_{DP}^* power law at 13 GHz appears to be slightly more biased than the (A_{H-V}, Φ_{DP}) method proposed here although this difference is small and becomes indistinguishable at 3 GHz. The least biased estimators are (A_{H-V}, Φ_{DP}) at 13 GHz and both (Z_{DR}, Φ_{DP}) as well as (Z_{DR}, Z_H) at 3 GHz. Similarly (Fig. 8b), ϵ_S is largest for the Z–W and W–A_H relations. For the other algorithms the ϵ_S are comparable, generally showing decreasing scatter with increasing D_m. Consequently, addition of the magnitudes of ϵ_S and ϵ_B (Fig. 8c) shows that in the absence of measurement errors (A_{H-V}, Φ_{DP}) at 13 and 3 GHz as well as (Z_{DR}, Φ_{DP}) and (Z_{DR}, Z_H) at 3 GHz are all clearly superior to Z–W and W–A_H relations and even to the W–Φ_{DP}^* relation at 13.8 GHz.

When measurement errors are included, however, several differences appear. First, it is worth noting that generally the algorithms at 13 and 9 GHz are superior to those at 3 GHz (Fig. 9). To a large degree this is due to the increased accuracy of estimating Φ_{DP} and A_{H-V} at these higher frequencies. Second, it appears that the method proposed here is generally superior to W–Φ_{DP}^* power laws at 13 and 3 GHz. Third, algorithms that require Z_H such as the Z–W and (Z_{DR}, Z_H) algorithms at 3 GHz are substantially degraded by an inability to measure Z with sufficient accuracy. Consequently, even though the (Z_{DR}, Z_H) algorithm is, in principle, quite good (Fig. 8), in practice its potential is severely compromised by having to include Z_H.

4. An example

To embody much of the theoretical discussions in the previous section, an analysis of measurements in a tropical rainstorm are presented next. These data were collected in 1991 during the Convection and Precipitation Experiment (CaPE) centered on the National Aeronautics and Space Administration (NASA) Kennedy Space Center in Florida. The National Center for Atmospheric Research (NCAR) CP-2 radar was especially equipped by Colorado State University (CSU) under NASA support for this project to gather propagation differential phase measurements at 3 GHz

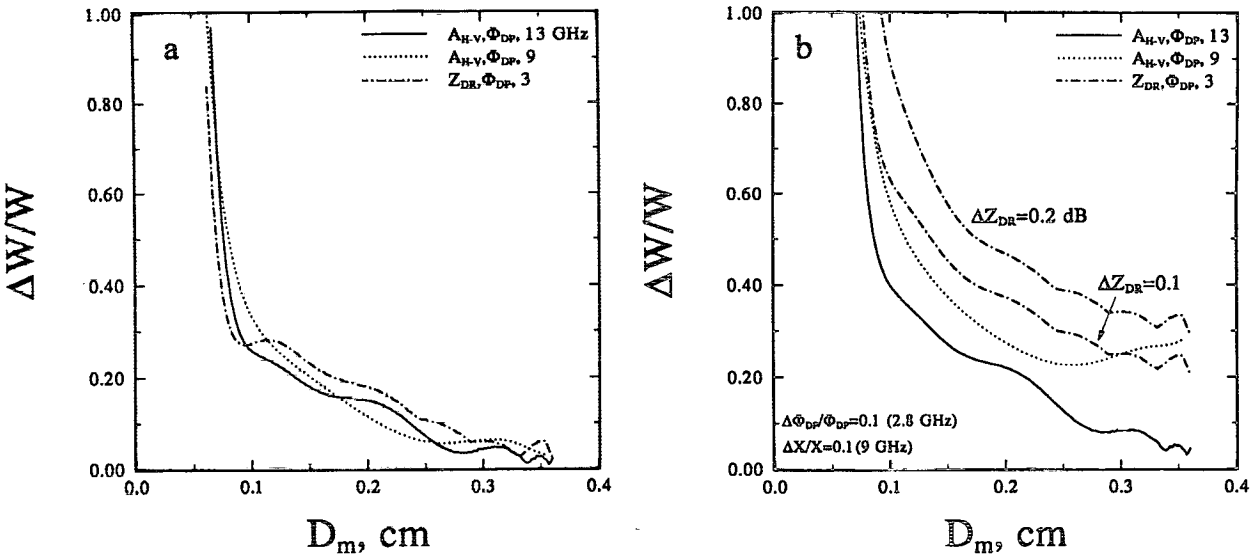

FIG. 6. The average fractional error of the estimate of the rainwater content for the indicated algorithms (a) excluding measurement errors but including scatter about the algorithms for D_m and Φ_{DP}/W and (b) including measurement errors as indicated and discussed further in the text.

(Chandrasekar et al. 1993). In addition, this radar system measures Z_{DR} at 3 GHz as well as the co- and cross-polarized radar reflectivity factors (Z_c and Z_x, respectively) at 9.34 GHz using an X-band component transmitting at horizontal polarization. However, because the incoherent 9-GHz radar could not switch between horizontal and vertical polarizations, neither Z_{DR} nor Φ_{DP} could be measured at this frequency.

Before proceeding, however, it is necessary first to consider how Φ_{DP} and A_{H-V} can be estimated. While it is a fairly simple matter, in principle, to measure parameters such as Z and Z_{DR}, Φ_{DP} and A_{H-V} cannot be measured directly but instead must be computed as the derivative with increasing distance from the radar of the measured accumulated propagation differential phase shift φ_{DP} and polarization differential attenuation. This latter quantity appears as a monotonic decreasing component of Z_{DR} (Jameson 1994a). While Z_{DR} at 9 GHz is not available using the CP-2 radar, it is possible, in principle, to estimate A_{H-V} from the monotonic increasing component of LDR = 10 $\log_{10}(Z_x/Z_c)$ (Jameson 1994a). In practice, however, this is very difficult to accomplish because A_{H-V} is the small residual of the difference between large numbers, residuals strongly affected by slight beam misalignments, signal fluctuations, and other factors. Consequently, in this study A_{H-V} could not be estimated successfully at 9 GHz. In this example, only 3-GHz observations of Z_{DR} and Φ_{DP} estimated according to the procedure in the Appendix are available for analysis.

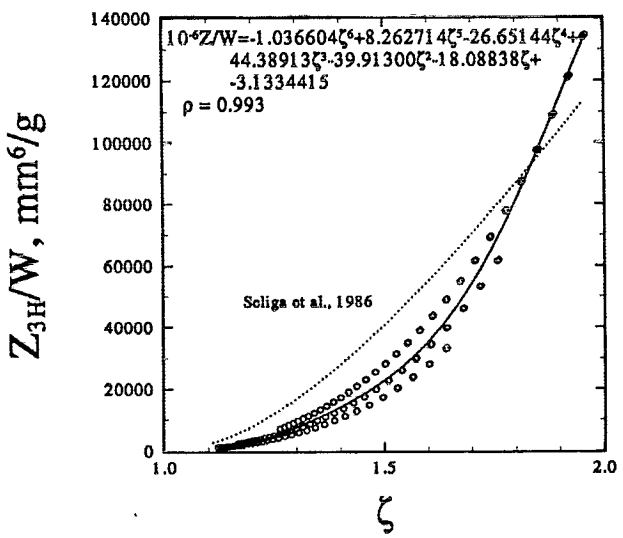

FIG. 7. The ratio of the reflectivity factor for horizontal polarization at 2.80 GHz to W as a function of ζ. A least-squares-error polynomial fit is performed to reduce potential bias errors that would result from using the formulation in Seliga et al. (1986) (dashed line).

The basic radar measurements in a rather average (Byers and Braham 1949), mature Florida summertime shower are shown in Fig. 10. Ancillary data indicate that the height of the 0°C level is at approximately 5 km, so that much of this shower is at temperatures above freezing. Most of the larger Φ_{DP} occur near and below this altitude. Significant Φ_{DP} are also coincident with the "core" of the shower defined by the larger reflectivity factors at 3 GHz, Z_{3H}. However, significant Φ_{DP} also occur at locations removed from where Z_{3H} is largest.

The most substantial Z_{DR} in Fig. 10 occur below an altitude of 3 km and largely coincide with the greatest Z_{3H}. Since Z_{DR} is a measure of the reflectivity factor–

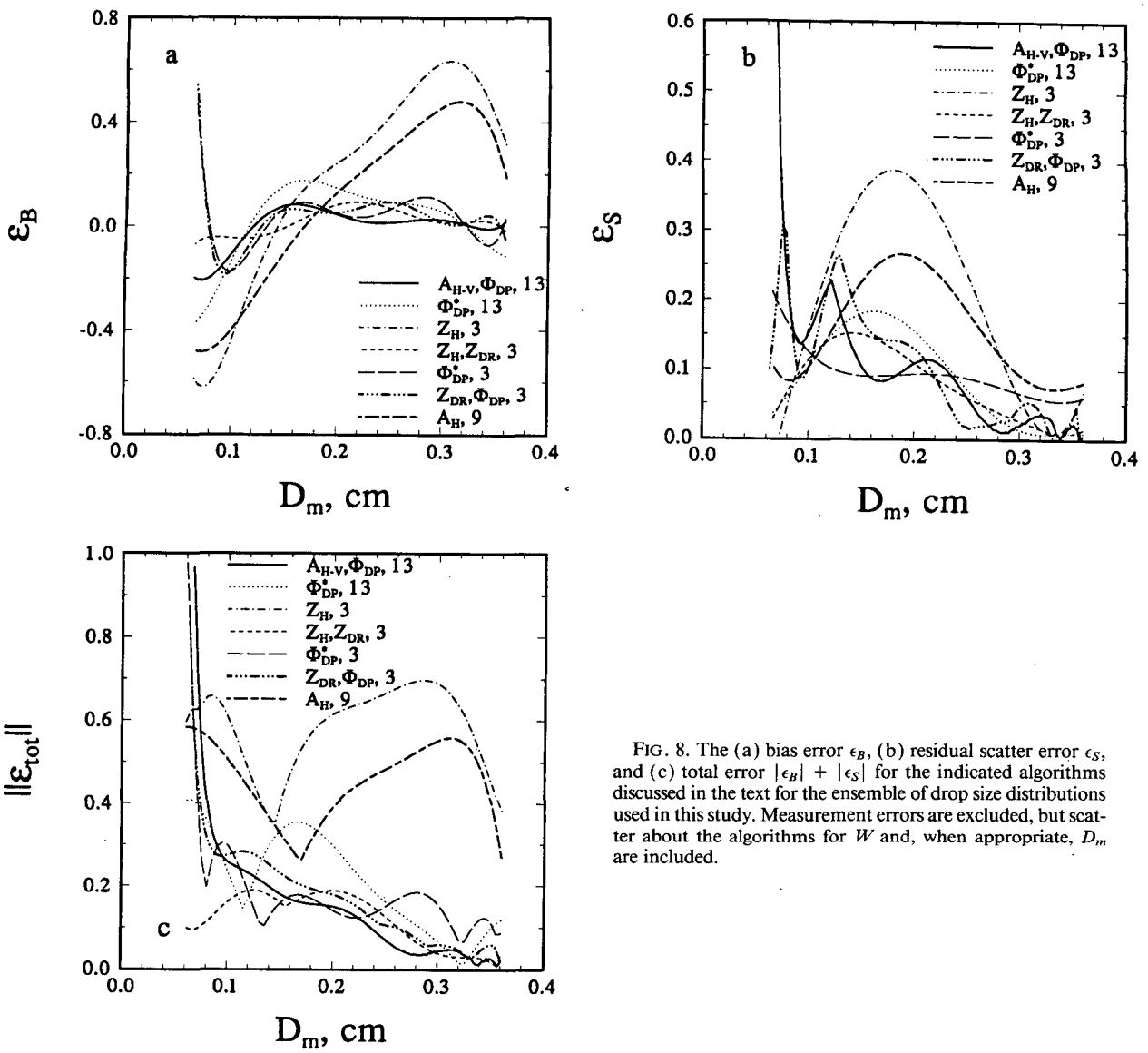

FIG. 8. The (a) bias error ϵ_B, (b) residual scatter error ϵ_S, and (c) total error $|\epsilon_B| + |\epsilon_S|$ for the indicated algorithms discussed in the text for the ensemble of drop size distributions used in this study. Measurement errors are excluded, but scatter about the algorithms for W and, when appropriate, D_m are included.

weighted mean raindrop axis ratio (Jameson 1983), the bigger the Z_{DR}, the larger the raindrops. More specifically, estimates of D_m computed from Z_{DR} are plotted in Fig. 11. In spite of some uncertainty in the exact values of Z_{DR} in this case, the spatial coincidence of the largest D_m and greatest Z_{3H} nevertheless strongly suggests that the reflectivity factor in these locations is significantly enhanced by the presence of large drops.

These Z_{3H} are also undoubtedly increased by a high concentration of rainwater as well. In fact estimates of W from Z using a power law imply that the rainwater contents are maximum precisely where the reflectivity factors are greatest. On the other hand, estimates of W using Φ_{DP} reveal an entirely different structure (Fig. 12) having the greatest values at altitudes of 3–4 km, considerably above the height of the maximum Z_{3H}. One plausible interpretation of these observations is that the largest, fastest falling raindrops are descending ahead of the bulk of the rainwater producing the largest values of Z_{DR} and Z_{3H} at lower levels, while most of the rain from this shower is yet to come.

Although this is only one, simple example, it exemplifies a potential importance of Φ_{DP}. *Specifically, Φ_{DP} decouples estimates of W [and the rainfall rate (R) as well] from Z.* This is advantageous for at least three reasons. First, the spatial and temporal structures of computed W and R no longer simply reflect those of the reflectivity factor, in contrast to what happens when using Z–R and Z–W relations. Second, because of this decoupling, it is possible to correlate Z with W and R over identical sampling volumes permitting the development of Z–R or Z–W relations useful for certain

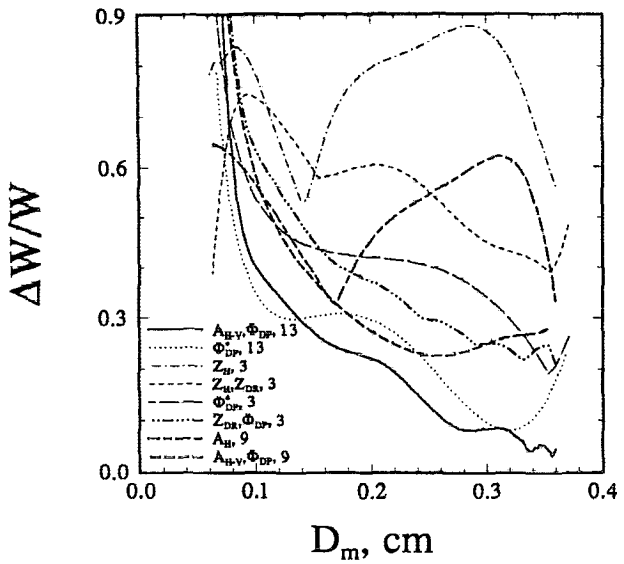

FIG. 9. The average fractional error of the estimate of W for several different radar estimators. Measurement errors are included as discussed in the text.

applications by conventional radars. Third, W and R can be estimated without the need for painstaking and often deficient absolute radar calibration required for as accurate as possible measurements of Z.

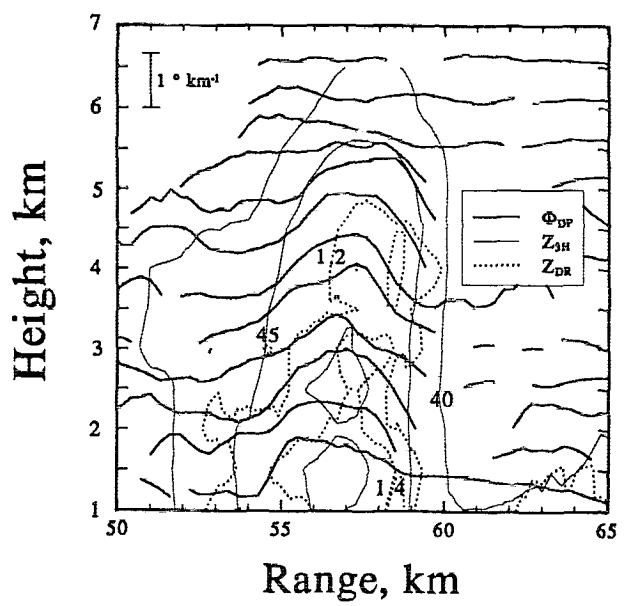

FIG. 10. Line plots of Φ_{DP} (deg km^{-1}) deduced at different elevation angles (altitudes) beginning at 1.08° (1.1 km at 60 km range) and spaced 0.42° (0.44 km at 60 km range) apart as a function of radar range. These are superimposed upon contour plots of the radar reflectivity factor (dBZ) at 3 GHz and horizontal polarization (Z_{3H}) and the 3-GHz differential reflectivity (dB) measured in a summertime Florida tropical rainstorm as part of the CaPE project. The height of 0°C is at about 5 km.

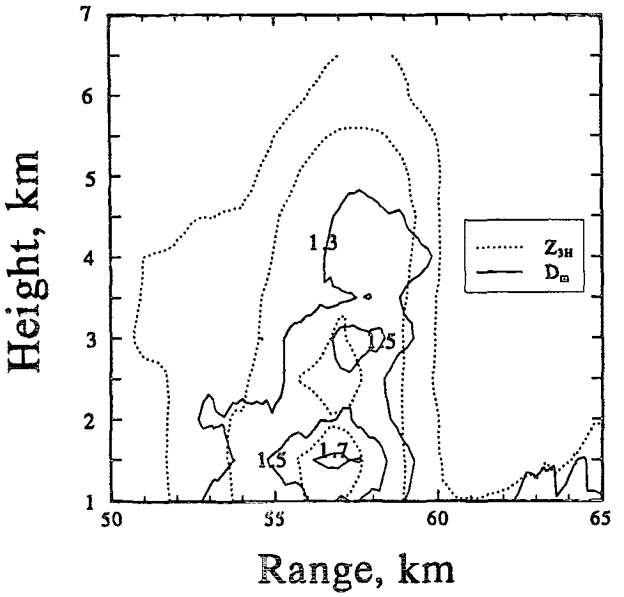

FIG. 11. The height structure of D_m (mm) deduced from Z_{DR} in Fig. 10 using the relation in Fig. 4. The largest drops are found below about 3 km.

5. Summary

This paper explains why the ratio of the specific polarization differential phase shift Φ_{DP} to the rainwater content W at several frequencies is nearly linearly related to the mass-weighted mean drop size D_m over a large domain. Consequently, W can be estimated from

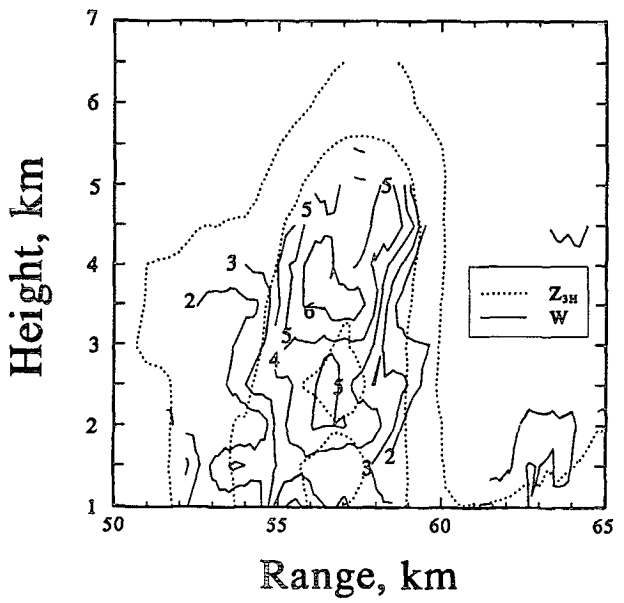

FIG. 12. The height structure of the rainwater content (g m^{-3}) deduced from Φ_{DP} in Fig. 10 and D_m in Fig. 11. Note that much of the rainwater lies above 3 km at this time.

Φ_{DP} using D_m derived from measurements of Z_{DR} at nearly nonattenuating frequencies or from the specific polarization differential attenuation A_{H-V} estimated using measurements of Z_{DR} at attenuating frequencies.

A study of the fractional errors of the estimate of W for an assumed ensemble of several different gamma drop size distributions, range of temperatures, and three frequencies (2.80, 9.34, 13.80 GHz) suggests that this approach yields results superior to classical and other polarization techniques for estimating the rainwater content, particularly those requiring the measurement of the reflectivity factor. Best results appear most likely at the highest frequency in part because of the anticipated greater accuracy of estimates of both Φ_{DP} and A_{H-V}.

Nevertheless, when it is of prime concern to collect measurements over the longest possible distances, transmissions at 3 GHz may be preferred to those at 13 GHz, which at times may attenuate below the detectable signal level. A dual-frequency (e.g., 3 and 13 GHz) radar probably provides the best combination of greatest accuracy and measurement distance.

The potential advantages of estimating W from Φ_{DP} are well illustrated in the example from the CaPE project. One of the most important is that such estimates are now no longer welded to the reflectivity factor as they are when using Z–R and Z–W relations. Consequently, temporal and spatial structures of W and R no longer must simply reflect those of Z. Specifically, as this example illustrates, the largest rainwater contents are no longer forced (e.g., by a Z–W power law) to occur where Z is greatest. A second important advantage of this new freedom is that since the estimates of W and R are based upon the rate of change of parameters with increasing distance (or on the ratios of reflectivity factors), it is no longer crucial to have an absolute calibration of the radar, a tedious and often inconclusive task at best. This is not to imply, however, that the measurements still do not require care using well-maintained and modern equipment.

Acknowledgments. The contribution to this paper by Jameson was funded in part by grants from NASA through the Goddard Space Flight Center (NAS5-30430) and by the Jet Propulsion Laboratory (JPL958437). Partial support was also provided by the National Science Foundation (NSF) through Grant ATM90-15394. Support for Caylor was provided by NSF Grant ATM-9014600. In addition, the authors gratefully acknowledge Prof. V. N. Bringi of the Electrical Engineering Department at Colorado State University for his support of this analysis and to both Profs. Bringi and V. Chandrasekar for their assistance in developing the processor for measuring the propagation differential phase shift. We are also grateful to Mr. Otto Thiele at NASA Goddard Space Flight Center whose support was crucial for developing the processor and collecting the data.

APPENDIX

Estimating Φ_{DP}

a. Theory

Although it is practically impossible to measure the absolute phases of backscattered signals at horizontal and vertical polarizations, in practice one can measure the total differential phase shift ψ between them. This phase consists of a propagation and a backscatter term (Jameson 1985), so that

$$\Psi = \varphi_{DP} + \delta_b, \tag{A1}$$

where φ_{DP} is the differential propagation phase shift $(\varphi_H - \varphi_V)$ and δ_b is the differential phase shift upon backscatter $(\delta_H - \delta_V)$.

For S-band measurements and nearly Rayleigh–Gans scatterers composed entirely of water, δ_b is small, typically less than 0.2° in rain (Jameson and Mueller 1985). Although ψ analyzed in this example may contain contributions from hail and ice near the melting level, the focus of this paper is on estimates of W computed at temperatures well above 0°C when δ is probably negligible. However, it is worth noting that where melting is occurring, the backscatter component may be estimated and removed from ψ if desired using a more sophisticated but slower signal-processing algorithm (Hubbert 1992) than the one used in this analysis.

The general technique for calculating φ_{DP} using a dual-polarization radar is described in Mueller (1984), while a rigorous treatment of estimator statistics is presented in Sachidananda and Zrnić (1986a). However, in these techniques care must be taken to account properly for phase ambiguities, that is, those instances when the phase wraps around a full cycle, typically at ±180° (Sachidananda and Zrnić 1986b). In this analysis, an algorithm using the pulse-pair covariances (Hubbert et al. 1993) is implemented to process such wraps.

When δ_b is negligible, the one-way specific differential propagation phase shift Φ_{DP} is simply the range derivative of the differential propagation phase shift (Jameson 1985; Bringi et al. 1990)

$$\Phi(r) = \frac{1}{2}\left.\frac{d\varphi_{DP}}{dr}\right|_0^r, \tag{A2}$$

where r is the radar range. Letting Δ be an increment in range on either side of r, this parameter may be estimated from

$$\mathcal{E}[\Phi(r)]_{DP} = \frac{1}{2}\frac{\varphi_{DP}(r-\Delta) - \varphi_{DP}(r+\Delta)}{2\Delta}. \tag{A3}$$

b. An example application

Figure A1a illustrates φ_{DP} as a function of range measured using the Colorado State University proces-

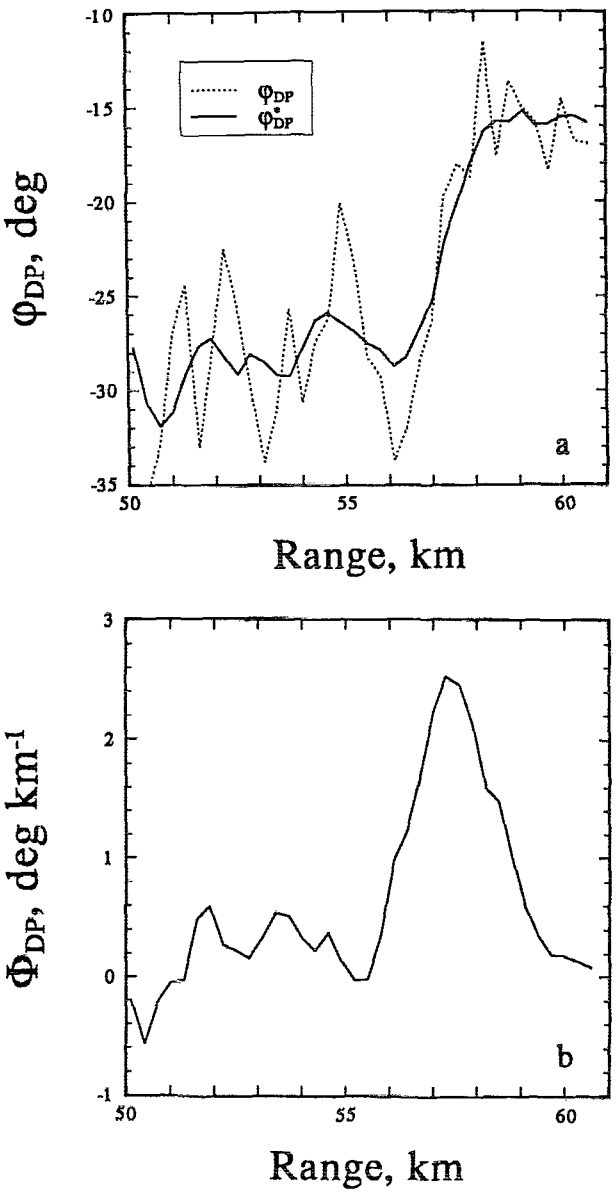

FIG. A1. (a) The unfiltered φ_{DP} (dashed) and seven-gate running average smoothed φ^*_{DP} (solid) as a function of distance from the radar in a Florida storm on 20 September 1991. (b) The estimated Φ_{DP} computed using a finite-difference estimator applied to φ^*_{DP} in (a). Here, Φ_{DP} is also smoothed using a seven-gate running average.

sor. Because φ_{DP} contains sharp statistical fluctuations, a robust algorithm must be used to estimate Φ_{DP}. A typical algorithm involves smoothing, or filtering, φ_{DP} prior to computing the derivative (Bringi et al. 1990; Jameson 1994a). Depending on the application, the resulting Φ_{DP} may also require filtering, particularly when the signal and noise levels are comparable.

The algorithm used to compute Φ_{DP} in this paper is a slightly modified three-step procedure originally described by Jameson (1994a). Specifically, in the first step a running average (boxcar filter) is applied to the φ_{DP} data. Thus, at each range, φ_{DP} is replaced by

$$\varphi^*_{DP}(r) = \frac{1}{2m+1} \sum_{r=-m}^{m} \varphi_{DP}(r), \qquad \text{(A4)}$$

where $m = 3$, a total width of 2.1 km for the range gate spacing of 300 m for these data. An example of φ^*_{DP} after filtering is shown (solid line) in Fig. A1a.

In the second step, Φ_{DP} is computed using (A3). As discussed by Jameson (1994a), Δ is not fixed but is allowed to vary from gate to gate subject to the criterion

$$\left| \frac{\varphi(r-\Delta)_{DP} + \varphi(r+\Delta)_{DP}}{2} - \varphi(r)_{DP} \right| \leq \gamma, \qquad \text{(A5)}$$

where γ is taken to be 1.0° in this example. When φ_{DP} is relatively noise free, a variable Δ improves the accuracy of the estimated Φ_{DP} by using as large a distance as possible while maximizing the difference in φ_{DP}. In the final, third step, Φ_{DP} is averaged according to (A4) with $m = 3$. Figure A1b illustrates the final estimated Φ_{DP} corresponding to the data in Fig. A1a.

REFERENCES

Atlas, D., 1964: Advances in radar meteorology. *Advances in Geophysics,* Vol. 10, 317–478.

——, and C. W. Ulbrich, 1974: The physical basis for attenuation–rainfall relationships and the measurement of rainfall parameters by combined attenuation and radar methods. *J. Rech. Atmos.*, **8,** 275–298.

Bringi, V. N., V. Chandrasekar, N. Balakrishnan, and D. S. Zrnić, 1990: An examination of propagation effects in rainfall on radar measurements at microwave frequencies. *J. Atmos. Oceanic Technol.*, **7,** 829–840.

Byers, H. R., and R. R. Braham, 1949: *The Thunderstorm.* U.S. Government Printing Office, 287 pp.

Chandrasekar, V., V. N. Bringi, N. Balakrishnan, and D. S. Zrnić, 1990: Error structure of multiparameter radar and surface measurements of rainfall. Part III: Specific differential phase. *J. Atmos. Oceanic Technol.*, **7,** 621–629.

——, G. R. Gray, and I. J. Caylor, 1993: Auxiliary signal processing system for a multiparameter radar. *J. Atmos. Oceanic Technol.*, **10,** 428–431.

Eccles, P. J., and E. A. Mueller, 1971: X-band attenuation and liquid water content estimation by a dual-wavelength radar. *J. Appl. Meteor.*, **10,** 1252–1259.

Hubbert, J., 1992: Radar polarimetry: Theory, analysis, and applications. Ph.D. Thesis, Department of Electrical Engineering, Colorado State University, 226 pp.

——, I. J. Caylor, V. Chandrasekar, 1993: A practical algorithm for the estimation of Doppler velocity and differential phases from dual polarized radar measurements. *26th Conf. on Radar Meteorology,* Norman, OK, Amer. Meteor. Soc., 112–117.

Jameson, A. R., 1983: Microphysical interpretation of multiparameter radar measurements in rain. Part I: Interpretation of polarization measurements and estimation of raindrop shapes. *J. Atmos. Sci.*, **40,** 1792–1802.

——, 1985: Microphysical interpretation of multiparameter radar measurements in rain. Part III: Interpretation and measurement of differential phase shift between orthogonal linear polarizations. *J. Atmos. Sci.*, **42,** 607–614.

——, 1989: Theoretical analysis and meteorological interpretation of the role of raindrop shape on microwave attenuation and propagation phase shifts: Implication for the radar measurement of rain. *J. Atmos. Oceanic Technol.*, **6,** 76–88.

——, 1991: A comparison of microwave techniques for measuring rainfall. *J. Appl. Meteor.*, **30,** 32–54.

——, 1992: The effect of temperature on attenuation correction schemes in rain using polarization propagation differential phase shift. *J. Appl. Meteor.*, **31,** 1106–1118.

——, 1994a: Measuring rainwater content by radar using propagation differential phase shift. *J. Atmos. Oceanic Technol.*, **11,** 299–310.

——, 1994b: An alternative approach to estimating rainfall rate by radar using propagation differential phase shift. *J. Atmos. Oceanic Technol.*, **11,** 122–131.

——, and E. A. Mueller, 1985: Estimation of differential phase shift from sequential orthogonal linear polarization radar measurements. *J. Atmos. Oceanic Technol.*, **2,** 133–137.

Mueller, E. A., 1984: Calculation procedures for differential propagation phase shift. *22d Conf. on Radar Meteorology,* Zurich, Amer. Meteor. Soc., 397–399.

Oguchi, T., 1973: Attenuation and phase rotation of radio waves due to rain: Calculations at 19.3 and 34.8 GHz. *Radio Sci.*, **8,** 31–38.

Pruppacher, H. R., and K. V. Beard, 1970: A wind tunnel investigation of the internal circulation and shape of water drops falling at terminal velocity in air. *Quart. J. Roy. Meteor. Soc.*, **96,** 247–256.

Sachidananda, M., and D. S. Zrnić, 1986a: Differential propagation phase shift and rainfall rate estimation. *Radio Sci.*, **21,** 907–922.

——, and ——, 1986b: Characteristics of echoes from alternately polarized transmission. Report 71, Cooperative Institute for Mesoscale Meteorological Studies, Norman, OK, 54 pp.

Sekhon, R. S., and R. C. Srivastava, 1971: Doppler radar observations of drop-size distributions in a thunderstorm. *J. Atmos. Sci.*, **28,** 983–994.

Seliga, T. A., and V. N. Bringi, 1976: Potential use of radar differential reflectivity measurements at orthogonal polarizations for measuring precipitation. *J. Appl. Meteor.*, **15,** 69–76.

——, and ——, 1978: Differential reflectivity and differential phase shift: Applications in radar meteorology. *Radio Sci.*, **13,** 271–275.

——, K. Aydin, and H. Direskenell, 1986: Disdrometer measurements during an intense rainfall event in central Illinois: Implications for differential reflectivity observations. *J. Climate Appl. Meteor.*, **25,** 835–846.

Ulbrich, C. W., 1983: Natural variations in the analytic form of the raindrop size distribution. *J. Climate Appl. Meteor.*, **22,** 1764–1775.

Van de Hulst, C. H., 1957: *Light Scattering by Small Particles.* Wiley and Sons, 470 pp.

Warner, C., and A. Hizal, 1976: Scattering and depolarization of microwaves by spheroidal raindrops. *Radio Sci.*, **11,** 921–930.

Waterman, P. C., 1965: Matrix formulation of electromagnetic scattering. *Proc. IEEE.*, **53,** 805–812.